Intermittent trapping of a liquid-like vortex state visualised by scanning Hall probe microscopy

A. Crisan[1,2,3], S. J. Bending[1], Z. Z. Li[4], H. Raffy[4]

[1] *Department of Physics, University of Bath, Claverton Down, Bath BA2 7AY, UK*

[2] *School of Metallurgy and Materials, University of Birmingham, Edgbaston, Birmingham B15 2TT, UK*

[3] *National Institute of Materials Physics, PO Box MG-7, Bucharest 077125, Romania*

[4] *Laboratoire de Physique des Solides, Bâtiment 510, UMR 8502, Université Paris-Sud, 91405 Orsay, France*

PACS 74.25.Uv – Vortex phases

PACS 74.25.Ha – Magnetic properties including vortex structures and related phenomena

PACS 74.25.Wx – Vortex pinning

Abstract

We have used scanning Hall probe microscopy to investigate vortex structures and vortex dynamics in $Bi_2Sr_2CaCu_2O_{8+\delta}$ thin films in very low perpendicular magnetic fields. After nominally zero field cooling in the earth's field we find that the vortices appear to be in a stable glassy state in our highly disordered samples. After applying a cancellation field of a few Oersted at low temperature, however, the system enters a new regime at very low magnetic induction when the only image contrast is due to vortices that are intermittently trapped on strong pinning centres. This state shares many of the signatures of the re-entrant vortex liquid phase that has been theoretically predicted in these highly anisotropic materials at very low vortex densities. Analysing the trapping times for vortices in the fluctuating state we estimate that the pinning potential of typical strong pinning centres is about 900 K under our experimental conditions. To our knowledge, this is the first direct experimental evidence for the existence of a dynamic liquid-like vortex state in this highly anisotropic material at very low magnetic induction.

1. Introduction

It is now well established that the vortex solid in layered cuprate superconductors can undergo a high field first order melting transition to a vortex liquid state, as proven experimentally [1-7] and discussed theoretically [8-10]. This phenomenon is particularly pronounced in the highly anisotropic material $Bi_2Sr_2CaCu_2O_{8+\delta}$ (Bi:2212) in which the melting line occurs at rather low fields in optimally doped samples (H_z < 400Oe), with H_z perpendicular to the CuO_2 planes. Melting in layered superconductors has been studied in the framework of Lindemann melting by Blatter *et al.* [11], and these authors point out that there should actually be two melting lines; the usual one at higher fields driven by short wavelength (k_z>1/λ) soft tilt modes of the lattice

$$B_m^u(T) \approx \frac{\Phi_0}{\lambda^2}\frac{\pi c_L^2}{4\sqrt{\beta}}\frac{\varepsilon_0 \varepsilon \lambda}{T} \propto \left(1-\frac{T^2}{T_c^2}\right)^{3/2} \quad , \qquad (1)$$

and a second "re-entrant" melting line driven by long wavelength fluctuations at very low fields when the lattice shear modulus becomes exponentially small:

$$B_m^l(T) \approx \frac{\Phi_0}{\lambda^2}\frac{1}{4}\left[\ln\left(\frac{4\pi c_L^2}{(3\pi)^{1/4}}\frac{\varepsilon_0 \lambda}{T}\right)\right]^{-2}. \qquad (2)$$

In eqns. (1) and (2), Φ_0 is the flux quantum, λ denotes the in-plane London penetration depth, c_L is the Lindeman constant (taken here and in Ref. 9 as 0.1), $\varepsilon_0=(\Phi_0/4\pi\lambda)^2$ denotes the vortex line energy, ε (<1) the effective mass anisotropy parameter, and $\beta=1/\ln(1+4\lambda^2/(c_L a_0)^2)$, where a_0 is the vortex lattice spacing.

These transition lines are plotted in Fig. 1 for the parameters of optimally doped Bi:2212. While the high field branch has been convincingly observed by a variety of techniques [1-7] the predicted low field re-entrant line has proved very difficult to identify experimentally for a number of reasons. It only occurs at very low values of magnetic induction which can be difficult to realise in bulk superconducting samples due to the steep slope of $B(H)$ near H_{c1}. In addition, a very low density of vortices is involved and any signatures of melting are inevitably weak and in competition

with quenched (pinning) disorder in the sample. Moreover, no direct imaging techniques exist with sufficient spatial and temporal resolution to track vortices in the liquid state. However, a careful analysis of fluctuation broadened profiles at very low fields in the Bragg glass phase of Bi:2212 single crystals has given indications for a second melting transition [12]. Estimated fluctuation amplitudes were found to show a minimum at intermediate applied fields and then grow again at very low fields suggestive of an approaching low field melting line.

Here we present results of vortex imaging studies that show strong evidence for a fluctuating liquid-like vortex state at low magnetic induction in a Bi:2212 thin film. Very large demagnetisation factors in our thin film geometry make it much easier to establish low density vortex distributions at low magnetic induction in nominally zero field-cooling experiments. Furthermore, our thin films are quite highly disordered with a low density of relatively strong vortex pinning sites. This turns out to be an advantage as we are able to verify the presence of vortices in the low field liquid-like state due to their intermittent trapping and de-trapping at a few strong pinning sites, during which time they become visible to our relatively low bandwidth imaging experiments.

2. Experimental Method

The 800nm thick Bi:2212 thin film was grown epitaxially on a heated $SrTiO_3$ substrate by single-target reactive rf magnetron sputtering. After deposition the film was cooled down under process gas, resulting in a slightly overdoped sample, with a critical temperature T_c (midpoint) of about 85 K, and a rather wide resistive transition $\Delta T \sim 20$ K (90% - 10% criterion), due to the high degree of disorder induced by sputter deposition and the relatively large film thickness. θ-2θ XRD patterns confirm that the film is single phase and *c*-axis oriented, and the full width at half maximum of the rocking curves, which characterizes the misorientation of the *c* axis, is 0.58°.

The Scanning Hall Probe Microscope (SHPM) used is a modified commercial low temperature STM in which the usual tunnelling tip has been replaced by a microfabricated GaAs/AlGaAs heterostructure chip. Electron beam lithography and wet chemical etching were used to define a 0.6 μm Hall probe in the two-dimensional electron gas approximately 5 μm from the corner of a deep mesa etch, which was coated with a thin Au layer to act as an integrated STM tip. The sensor was driven with a 20μm dc current and typical self-fields at the sample are of the order of a few tens of microgauss, much too small to perturb the measured vortex system. The sample was first approached towards the sensor until tunnelling was established and then retracted about 100-200 nm to allow rapid scanning without height feedback control. The Hall probe subtends an angle of about 1° with the sample plane so that the STM tip is always the closest point to the surface, and the Hall sensor was typically ~500-700 nm above the sample during imaging. The temperature-dependent scan field, which is ~21μm×21μm at 59K (the temperature of the experiments shown here), is divided into 128×128 pixels. Scans start at the bottom left hand corner of all images shown and move initially to the right, hence the horizontal x-axis represents the "fast scan" direction and the vertical y-axis the "slow scan" direction. A full 128×128 pixel scan was captured in about 6 seconds, and there was no significant delay between the end of one scan and the beginning of the next. The local magnetic induction at each pixel $B_{i,j}$ (i,j = 1-128) is an average of 13 consecutive measurements, resulting in a map of the local magnetic induction, B_{ij}, an average value of induction over the entire scan area, and a greyscale, ($B_{i,j}^{max}$-$B_{i,j}^{min}$). A more detailed description of the instrument and scanning technique is given elsewhere [13]. In principle our experimental set-up allows one to independently apply out-of-plane (H_z) and in-plane ($H_{||}$) fields generated by a vertically orientated solenoid and two pairs of orthogonal Helmholtz coils outside the cryostat. In practice, however, in the experiments described here we have only applied very low out-of-plane fields, H_z, in order to cancel the majority of the earth's magnetic field and obtain a rather low vortex density in our film.

3. Experimental Results

Fig. 2 shows a first set of SHPM images where each frame represents an average of 25 scans captured after nominal zero-field-cooling from 77K to 59K. In practice the sample would have been in a small field, ~-1Oe, during cooling due to a combination of the earth's field and stray static fields from nearby ferrous objects in the laboratory. Thermal contraction/expansion of the scanner head during heating and cooling demands that the Hall sensor be retracted some distance from the sample surface for safety, with the undesirable consequence that the reproducibility of the scan region and scan height is compromised during field-cooled imaging. To avoid these problems we did not change the temperature after the initial ZFC, and subsequent cancellation fields are all applied at 59K. Figures 2 a-e, present images captured for perpendicular applied fields H_z = 0, 1.2, 1.4, 1.6, 1.8 Oe respectively. Note that the sign of the applied field has been chosen to cancel the flux trapped while cooling in the earth's field. Moreover, since this field is applied at low temperatures when the J_c of the film is quite large, cancellation will be highly non-linear due to vortex pinning and the formation of a critical state within the film. Several black vortices are visible in Fig. 2a as expected for the negative sign of the stray magnetic field at the cryostat. Surprisingly, we also see two or three white vortices whose fields actually oppose the expected stray field direction. We speculate that these arise during earth field-cooling as Meissner screening effects turn on and the film tries to expel some of the flux trapped in it. In our thin film geometry these screening currents will lead to a strong field inversion at the sample boundary and it is easier for antivortices to penetrate the film from the edge than for strongly pinned vortices to leave the film from the bulk. Similar effects were reported previously in SHPM images on Bi:2212 single crystal platelets when the sign of applied field was reversed during field sweeps [14]. Figs.2b-e all look very similar to Fig. 2a, indicating that nearly all penetrating flux is trapped in Bean-like profiles near the sample edges outside the field of view at this low temperature. Eventually a further increase of H_z to 2.0 Oe (Fig. 2f) leads to several white vortices penetrating into the scanned area in

the top-right-hand corner of the image. At H_z =2.2 Oe (Fig. 2g) almost all of the black vortices have been annihilated, and two clear white vortices are seen with one remnant black one in the bottom-right hand corner. At 2.4 Oe no vortices are observed in the scanned frame while at 2.6 Oe (Fig. 2h) and 3 Oe (Fig. 2i) a few white vortices are seen whose number no longer increases systematically with increasing field (in the absence of screening we would expect an average increase of about 20vortices/Oe). Surprisingly, integration of the net flux associated with the well-isolated residual vortices observed indicated that it was less than a flux quantum, in some cases very considerably less. Detailed examination of the 25 individual scans that were averaged to create Figs. 2 h & i revealed that, contrary to expectation, the vortex patterns in sequential frames exhibited qualitative differences for the entire duration of the experiments (~2.5 mins). The rest of this paper is devoted to a systematic analysis of the unusual vortex dynamics observed in this regime.

At low applied fields (H_z<2 Oe at which the penetration of white vortices and subsequent black vortex annihilation occurs) we always observe stable vortex structures within our measurement bandwidth. Figure 3 shows a selection of 11 out of 25 consecutive scans, captured in a different zero field-cooling cycle to that of Fig. 2, after application of at an applied field of H_z=1.8 Oe. Also shown is the average image constructed from all 25 scans. Within the noise level of our system all frames appear to be identical indicating that, during the 2.5 minutes needed to complete the 25 scans, all the observed vortices remained trapped on rather strong pinning centres. The highly disordered nature of the images, and the apparent absence of vortex motion, suggests that the vortex system is in a stable glassy-state in this regime, although we cannot completely rule out that very rapid vortex fluctuations are occurring on timescales less than ~50ms (the time to scan one line of an image) which would be invisible to our experiment.

At very low values of local magnetic induction, when the field is increased just beyond the point where we have cancelled the remnant stray field at H_z=2.4 Oe, dramatic changes in successive images suggest very rapid vortex fluctuations. An example of this behaviour is shown in Fig. 4,

where we find that all the 25 consecutive scans captured at an applied field of H_z=3 Oe look qualitatively different. For example, in Fig. 4a there are no vortices in the frame, while in Fig. 4b one vortex appears trapped on the pinning centre labelled 1, and disappears again in Fig. 4c (each scan takes 6 seconds to capture). The vortex labelled 2 appears in frame 4d, is still present in frame 4e, but vanishes again in frame 4f. The vortex labelled 3, which appears in frame 4e, remains pinned for a somewhat longer time (c.f., Figs. 4e-h). Summarising the overall behaviour, we see many other vortices that appear in a given frame and remain pinned for durations ranging from 1-2 seconds for the "partial" vortices seen in figures 4m & 4y up to more than 50 seconds for the vortex labelled 4 in Figs. 4n-v). The trapping time for vortices on various strong pinning centres is also directly reflected in the amplitude of linescans across the average of all 25 frames as shown at the bottom of Fig. 4. The linescan across the pinning centres labelled 1 and 4 shows that the maximum induction corresponding to the pinning centre labelled 4 ("occupied" by a vortex in 12 frames) is approximately double that of the one corresponding to the pinning centre labelled 1 ("occupied" by a vortex in 5 frames). The correlation between the time spent on strong pinning sites and maxima in local induction can also be seen in the other linescan across pinning centres labelled 2 and 3.

4. Discussion

We speculate that the images shown in the 25 consecutive scans in Fig. 4 are indicative of a partially pinned liquid-like vortex state. . Similar, and possibly related behaviour was observed in Lorentz microscopy images of Bi2212 thin films by Tonomura for T>25K when vortices were seen to hop rapidly on and off pinning sites [15]. In this case, however, vortex motion was *driven* by gradually ramping up the applied field, and the thin film samples studied had been peeled from a single crystal and presumably had much lower levels of disorder. Although our nominally zero field cooled vortex system is not strictly in thermal equilibrium, it is interesting to compare our results with theoretical predictions for a thermodynamic re-entrant vortex liquid phase. The low temperature vortex system in a strongly pinning type II superconductor can, in practice, never truly

be in equilibrium anyway. Assuming that local flux cancellation is occurring at H_z~2.4Oe, we estimate that this fluctuating state exists at local magnetic inductions below ~1 G, in reasonable agreement with theoretical predictions for the re-entrant liquid in Bi2212 due to Blatter *et al.* [11]. Normally vortices in a liquid-like state would be invisible to our relatively low bandwidth imaging technique. However, due to the existence of a few strong pinning centres in our field of view, we are able to resolve occasional events when vortices become trapped for periods comparable to the 6s required to capture a single image. In slightly higher net magnetic inductions (c.f., Fig. 3) the vortex system may be considered to lie above the re-entrant melting line and become 'frozen'. We emphasise, however, that the stable configuration corresponds to a highly disordered glassy vortex state in our thin films, not the Bragg glass considered by Blatter et al. [11]. The starkly different dynamic behaviour for vortices in Figs. 3 and 4 in the absence of an external driving force represents the first direct evidence for a dynamic liquid-like vortex state in this highly anisotropic material at low magnetic induction which might be related to the low field 're-entrant' vortex liquid phase predicted for layered high-T_c superconductors [11].

Finally, in addition to experimental evidence for a liquid-like vortex state, an analysis of the lifetimes of trapped vortices before thermally-activated depinning allows a rough estimation of the pinning potential to be made. Knowing the time needed to complete one scan (6 s), we can estimate the time, τ, spent by vortices on their respective pinning centres. At these low values of magnetic induction our system is approximately in the isolated vortex regime ($a_0 << \lambda$) and the depinning process is expected to be a simple thermally-activated one described by $\tau=\tau_0 \exp(U/k_B T)$, where τ_0 is the inverse of the macroscopic attempt frequency (~10^6 Hz [16]) and U is the pinning potential of the individual pinning centre. Placing upper and lower bounds on the trapping time for many vortices captured in the liquid-like phase we estimate an average pinning potential, U_{av} = 900±100 K, which is quite reasonable for strong pinning centres in a Bi:2212 film at 59 K.

5. Conclusions

In conclusion, we have used scanning Hall probe microscopy to obtain the first direct evidence of a dynamic liquid-like vortex state in highly anisotropic Bi:2212 thin films at very low magnetic induction which might be related to the low field 're-entrant' vortex liquid phase predicted by Blatter *et al.* [9] over a decade ago. The dynamic behaviour of vortices that are intermittently trapped on strong pinning centres in the fluctuating state allows us to estimate the typical pinning for these sites in highly disordered Bi:2212 thin films.

Acknowledgements

The financial support of EPSRC (UK) through grant EP/E039944/1, the ESF-NES Network, the European Commission through a Marie Curie Excellence grant MEXT-CT-2006-041111 "NanoTechPinningHTS" and the Romanian Ministry of Education and Research is gratefully acknowledged.

References

[1] Lee S L, Zimmermann P, Keller H, Warden M, Savić I M, Schauwecker R, Zech D, Cubitt R, Forgan E M, Kes P H, Li T W, Menovsky A A and Tarnawski Z 1993 *Phys. Rev. Lett,* **71** 3862

[2] Cubitt R, Forgan E M, Yang G, Lee S L, Paul D McK, Mook H A., Yetiraj Kes P H, Li T W, Menovsky A A, Tarnawski Z and Mortensen K 1993 *Nature* (London) **365** 407

[3] Pastoriza H, Goffman M F, Aribére A and De La Cruz F 1995 *Phys. Rev. Lett,* **72** 2951

[4] Zeldov E, Majer D, Konczykowski M, Geshkenbein V B, Vinokur V M and Shtrikman H 1995 *Nature* (London) **375** 373

[5] Schilling A, Ott H R and Wolf T H 1992 *Phys. Rev*. B **46** 14 253

[6] Kwok W K, Fleshler S, Welp U, Vinokur V M, Downey J, Crabtree G W and Miller M M 1992 *Phys. Rev. Lett*. **69** 3370

[7] Safar H, Gammel P L, Huse D A, Bishop D J, Rice J P and Ginsberg D M 1992 *Phys. Rev. Lett*. **69** 824

[8] Nelson D R 1988 *Phys. Rev. Lett*. **60** 1973

[9] Houghton A, Pelcovits R A and Sudbø A 1990 *Phys. Rev*. B **40** 6763

[10] Fisher D S, Fisher M P A and Huse D A 1991 *Phys. Rev*. B **43** 130

[11] Blatter G, Geshkenbein V B, Larkin A I and Nordborg H 1996 *Phys. Rev*. B **54** 72

[12] Bending S J, Oral A, Kaya I I, Ooi S, Tamegai T and Henini M 1999 *IEEE Trans. Appl. Supercond*, **9** 1820

[13] Oral A, Bending S J and Henini M 1996 *Appl. Phys. Lett*. **69** 1324

[14] Dede M, Oral A, Yamamoto T, Kadowaki K and Shtrickman H 2006 *Jpn. J. Appl. Phys.* **3B** 2246

[15] Tonomura A 2007 *Physica* C **460-462** 285

[16] Blatter G, Feigel'man M V, Geshkenbein V B, Larkin A I and Vinokur V M 1994 *Rev. Mod. Phys.* **66** 1125

Figure Caption:

Fig. 1. Vortex phase diagram for a highly anisotropic superconductor showing the usual high field melting line and the low-field 're-entrant' melting line as predicted in Ref. 9, calculated using typical parameters for optimally doped Bi:2212 films. The coloured symbols linked by an arrow represent the phase space explored in this experiment.

Fig. 2. SHPM images of vortices in perpendicular applied fields, from (a) to (i), of 0, 1.2, 1.4, 1.6, 1.8, 2.0, 2.2, 2.6, and 3 Oe, with grayscales (GS) of 0.788, 0.797, 0.791, 0.766, 0.740, 0.865, 0.704, 0.723, 0.708 Gs. Each frame represents an average of 25 consecutive scans and the field of view is ~21μm×21μm. Note that total flux cancelation in the scanned region (with no resolvable vortices) occurred at an applied field of 2.4 Oe.

Fig. 3 A selection of 11 of 25 consecutive scans captured in a perpendicular applied field of 1.8 Oe showing a stable glassy vortex configuration. Bottom right; image shows the average of all 25 individual scans. In the scans GS values were between 0.78 and 0.92 Gs without any pattern in variation. All images have a field of view of ~21μm×21μm.

Fig. 4 Top: 25 consecutive SHPM images captured in a perpendicular applied field of 3 Oe, labeled with the time when each scan started. GS values were between 0.80 (no visible vortices) and 1.14 Gs. All images have a field of view of ~21μm×21μm. Numbers 1 to 5 indicate the positions of strong pinning centres that have trapped vortices for significant fractions of the 6s required to record a single scan. Bottom left image shows the average of all 25 individual scans, with arrows indicating the direction of the line-scans plotted in the graph on the bottom-right.

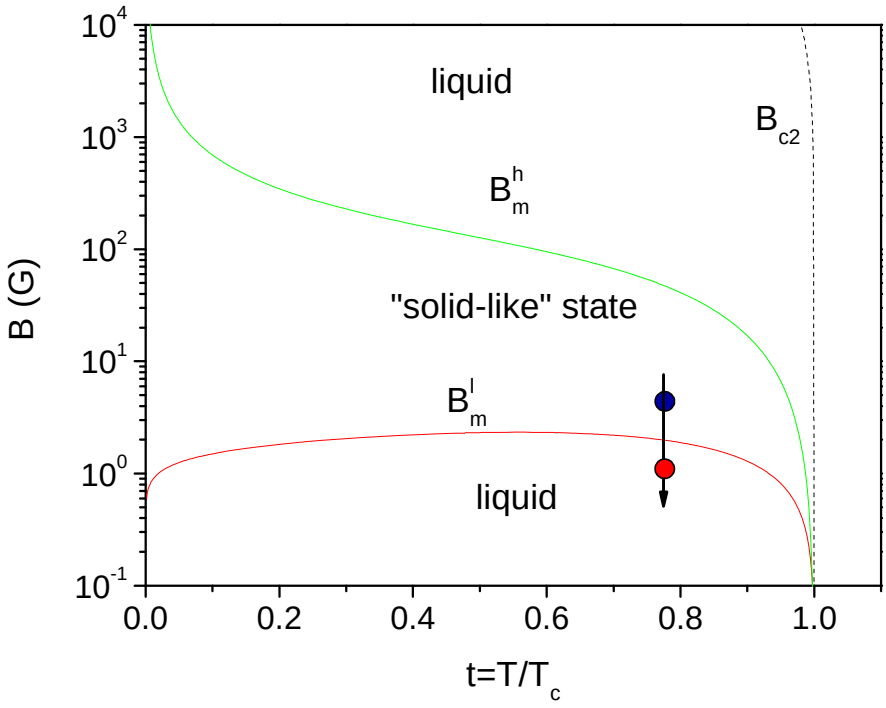

Fig. 1. Crisan et al.

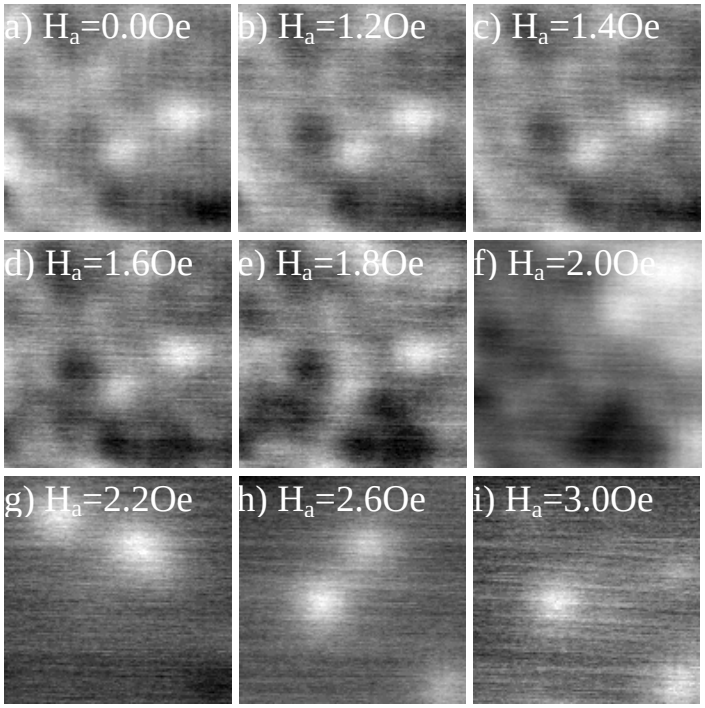

Fig. 2. Crisan et al.

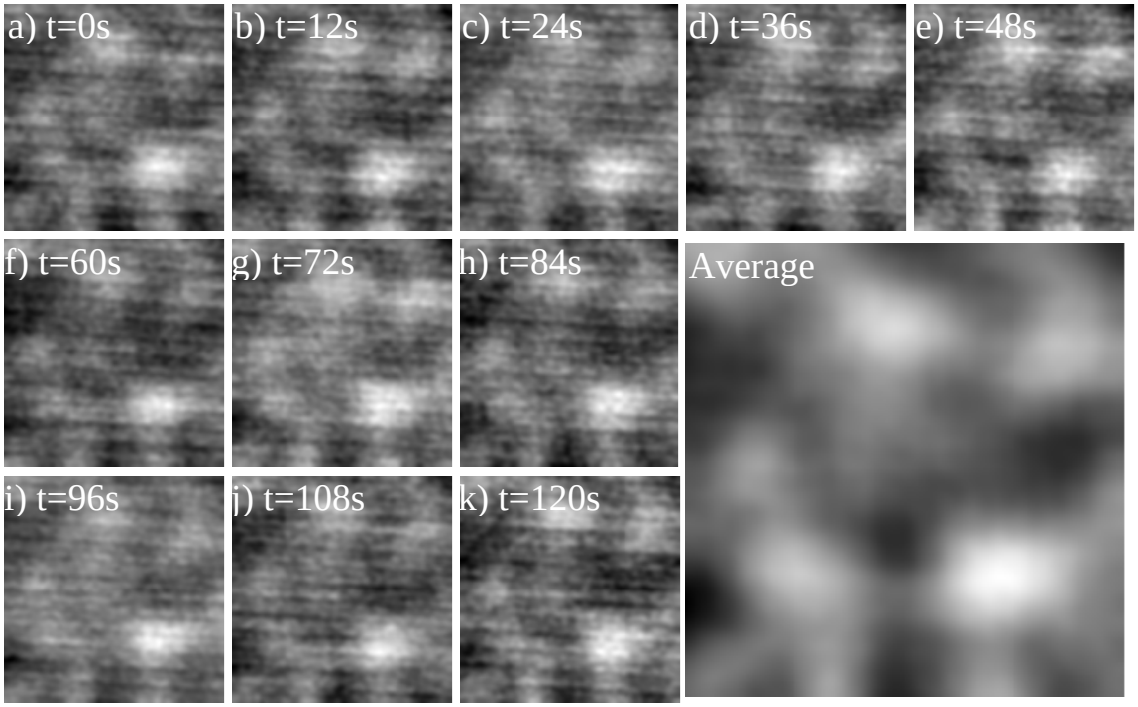

Fig. 3. Crisan et al

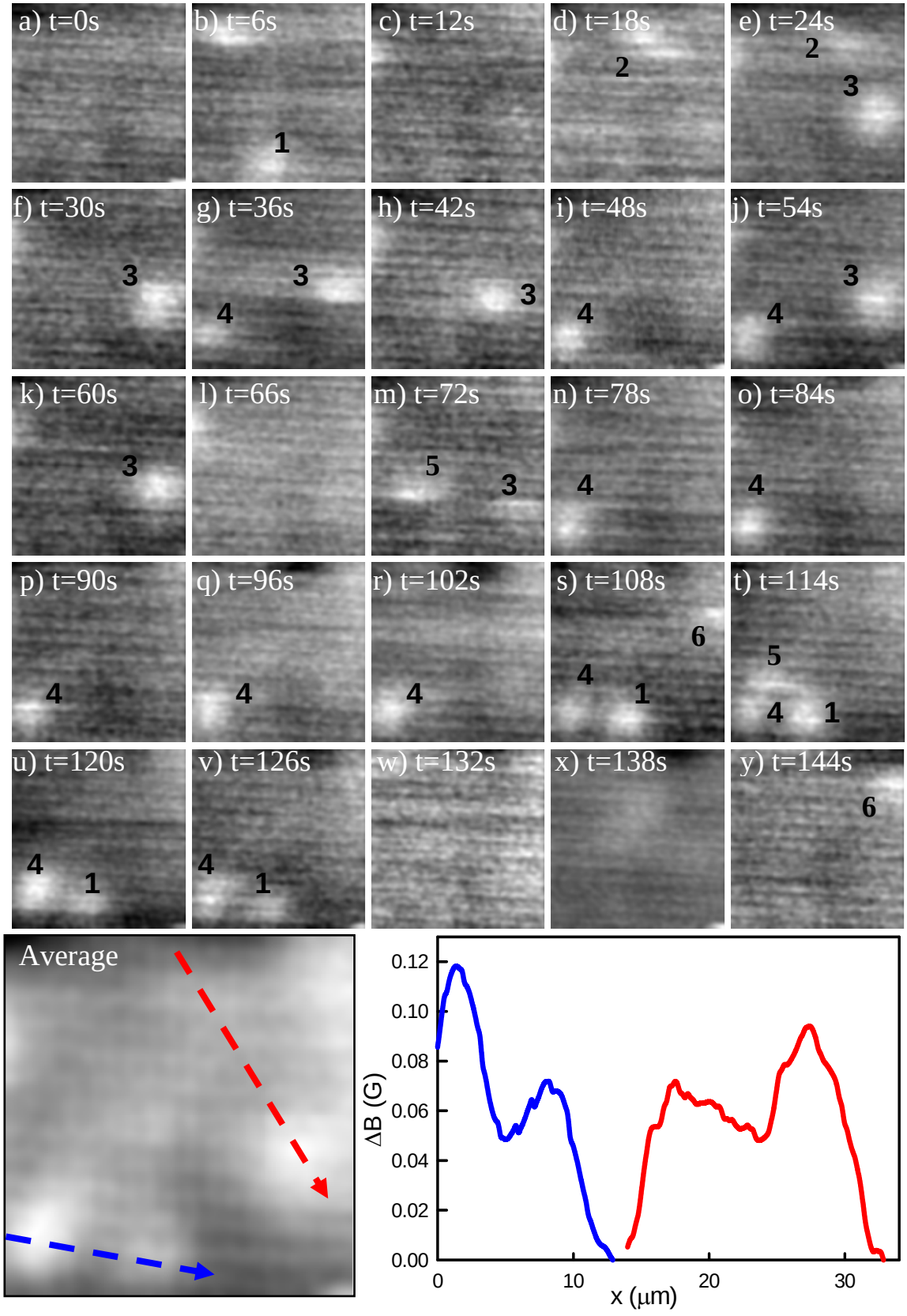

Fig. 4. Crisan et al.